

THE DISCOVERY OF PRIMEVAL LARGE-SCALE STRUCTURES  
WITH FORMING CLUSTERS AT REDSHIFT 6<sup>1</sup>MASAMI OUCHI<sup>2,3</sup>, KAZUHIRO SHIMASAKU<sup>4</sup>, MASAYUKI AKIYAMA<sup>5</sup>, KAZUHIRO SEKIGUCHI<sup>5</sup>,  
HISANORI FURUSAWA<sup>5</sup>, SADANORI OKAMURA<sup>4</sup>, NOBUNARI KASHIKAWA<sup>6</sup>, MASANORI IYE<sup>6</sup>,  
TADAYUKI KODAMA<sup>6</sup>, TOMOKI SAITO<sup>4</sup>, TOSHIYUKI SASAKI<sup>5</sup>, CHRIS SIMPSON<sup>7</sup>,  
TADAFUMI TAKATA<sup>5</sup>, TORU YAMADA<sup>6</sup>, HITOMI YAMANOI<sup>8</sup>,  
MAKIKO YOSHIDA<sup>4</sup>, AND MICHITOSHI YOSHIDA<sup>9</sup>*To Appear in the Astrophysical Journal Letters*

## ABSTRACT

We report the discovery of primeval large-scale structures (LSSs) including two proto-clusters in a forming phase at  $z = 5.7$ . We carried out extensive deep narrow-band imaging in the  $1 \text{ deg}^2$  sky of the Subaru/XMM-Newton Deep Field, and obtained a cosmic map of 515 Ly $\alpha$  emitters (LAEs) in a volume with a transverse dimension of  $180 \text{ Mpc} \times 180 \text{ Mpc}$  and a depth of  $\sim 40 \text{ Mpc}$  in comoving units. This cosmic map shows filamentary LSSs, including clusters and surrounding 10-40 Mpc scale voids, similar to the present-day LSSs. Our spectroscopic follow-up observations identify overdense regions in which two dense clumps of LAEs with a sphere of 1-Mpc diameter in physical units are included. These clumps show about 130 times higher star-formation rate density, mainly due to a large overdensity,  $\sim 80$ , of LAEs. These clumps would be clusters in a formation phase involving a burst of galaxy formation.

*Subject headings:* large-scale structure of universe — galaxies: clusters: general — galaxies: formation

## 1. INTRODUCTION

Recently, there has been a great progress in observational studies of structures of the high-redshift Universe. Steidel et al. (1998) found a proto-cluster at  $z = 3.1$  with a large population of Lyman break galaxies (LBGs). A significant excess of Ly $\alpha$  emitters (LAEs) was found by Venemans et al. (2002) around a radio galaxy at  $z = 4.1$ , and a subsequent study concluded that this excess is indeed a proto-cluster with a size of 3–5 Mpc (Miley et al. 2004). More recently, Venemans et al. (2004) reported clustering of 6 LAEs near a radio galaxy at  $z \sim 5.2$ . For structures beyond cluster scales, wide-field narrow-band surveys revealed very inhomogeneous distribution of LAEs (Ouchi et al. 2003; Shimasaku et al. 2003; Ajiki et al. 2003; Shimasaku et al. 2004; Hu et al. 2004) at  $z \simeq 5$ –6. Shimasaku et al. (2003) report an elongated overdense region of LAEs at  $z = 4.86$  on the sky of 20 Mpc in width and 50 Mpc in length. However, on the same sky, Shimasaku et al. (2004) found no large-scale structure at  $z = 4.79$  which is closer to us by 39 Mpc, indicating a large cosmic variance over their surveyed volumes. Although a few segments of high- $z$  structures have been found to date, the whole picture of high- $z$  Universe

is veiled. Moreover, we do not know when and how the structures of galaxies seen at present formed from the initial matter density fluctuations. We started a systematic survey to map the high- $z$  Universe with LAEs and LBGs at  $3 < z < 7$  in the  $1 \text{ deg}^2$  sky of the Subaru/XMM-Newton Deep Field (SXDF: R.A. =  $2^h 18^m 00^s$ , decl. =  $-5^\circ 00' 00''$  [J2000]; Sekiguchi et al. 2004). We obtained cosmic maps on scales of much larger than present-day LSSs to cover a network of LSSs at several redshifts between  $z = 3$  and 7. In this letter, we report the initial results of our survey about structures made of LAEs at  $z = 5.7$ . Throughout this paper, we adopt  $H_0 = 70 h_{70} \text{ km s}^{-1} \text{ Mpc}^{-1}$  and  $[\Omega_m, \Omega_\Lambda, n, \sigma_8] = [0.3, 0.7, 1.0, 0.9]$ .

## 2. PHOTOMETRIC SAMPLE

We carried out extensive deep narrow-band imaging on 2003 September 27-30 and October 22 with Subaru/Suprime-Cam (Miyazaki et al. 2002). We used the narrow-band filter NB816 whose central wavelength and FWHM are  $8150 \text{ \AA}$  and  $120 \text{ \AA}$ , respectively (Hayashino et al. 2003; Ajiki et al. 2003; Hu et al. 2004). This filter enables us to identify LAEs, galaxies with a strong Ly $\alpha$  emission line, at  $z \simeq 5.7 \pm 0.05$  with a small fraction of foreground contaminants (20-30%; e.g. Hu et al. 2004). Our 20-hour exposure imaging covered an area of  $1.04 \text{ deg}^2$  with 5 Suprime-Cam pointings. The sky was clear and the observational conditions were stable, with typical seeing sizes of  $0''.5$ – $0''.6$ . The data were reduced with a software package SDFRED (Yagi et al. 2002; Ouchi et al. 2004a). The sky noise of the reduced image is  $26.0 \pm 0.1 \text{ (AB)}$  at the  $5\sigma$  level with a  $1''.8$ -diameter circular aperture.

We detected 305,012 objects down to  $NB816 = 26.0$  with SExtractor (Bertin & Arnouts 1996) and measured their narrow-band excess color ( $i' - NB816$ ) and continuum color ( $R - i'$ ) by combining existing very deep  $R$ - and  $i'$ -band images of the SXDF (see Kodama et al. 2004).

<sup>1</sup> Based on data collected at Subaru Telescope, which is operated by the National Astronomical Observatory of Japan.

<sup>2</sup> Space Telescope Science Institute, 3700 San Martin Drive, Baltimore, MD 21218, USA; ouchi@stsci.edu.

<sup>3</sup> Hubble Fellow

<sup>4</sup> Department of Astronomy, School of Science, University of Tokyo, Tokyo 113-0033, Japan

<sup>5</sup> Subaru Telescope, National Astronomical Observatory, 650 N.A'ohoku Place, Hilo, HI 96720, USA

<sup>6</sup> National Astronomical Observatory, Tokyo 181-8588, Japan

<sup>7</sup> Department of Physics, University of Durham, South Road, Durham DH1 3LE, UK

<sup>8</sup> Department of Mathematical and Physical Sciences, Faculty of Science, Japan Women's University, Tokyo 112-8681, Japan

<sup>9</sup> Okayama Astrophysical Observatory, National Astronomical Observatory, Kamogata, Okayama 719-0232, Japan

Figure 1 shows the two color diagram of  $i' - NB816$  and  $R - i'$  for the  $NB816$  detected objects, together with colors of model galaxies and Galactic stars. In Figure 1, model LAEs at  $z = 5.7$  have very red colors both in  $i' - NB816$  and  $R - i'$  because of a strong Ly $\alpha$  emission line and a continuum trough at  $< 1216\text{\AA}$ , which are distinguished from colors of foreground objects. We defined the criteria for  $z \simeq 5.7 \pm 0.05$  LAEs as  $i' - NB816 > 1.0$  and  $R - i' > 0.7$ , and selected 515 LAEs from all the detected objects. These selection criteria isolate emission line objects with an observed-frame equivalent width of  $EW_{\text{obs}} \gtrsim 226\text{\AA}$  and a line flux of  $f \gtrsim 6.1 \times 10^{-18} \text{ erg s}^{-1} \text{ cm}^{-2}$ , if a flat continuum spectrum is assumed. The contamination rate of our LAE sample is estimated to be about 30% based on our spectroscopic follow-up observations described in section 3.2. The surface density and number density of these 515 LAEs are estimated to be  $\bar{\Sigma} = 0.14 \pm 0.01 \text{ arcmin}^{-2}$  and  $\bar{n} = 5.5 \pm 0.2 \times 10^{-4} \text{ Mpc}^{-3}$ . We also calculate the surface density down to the same magnitude limit as Hu et al. (2004) ( $NB816 < 25.05$ ) and obtain  $0.03 \text{ arcmin}^{-2}$  which is consistent with that of Hu et al. (2004).

### 3. RESULTS AND DISCUSSION

#### 3.1. Primeval Large-Scale Structures at $z = 5.7$

Figure 2 is the cosmic map showing the distribution of 515 LAEs at  $z = 5.7$  in the SXDF. The surveyed volume has a transverse dimension of  $180 \text{ Mpc} \times 180 \text{ Mpc}$  and a depth of  $\sim 40 \text{ Mpc}$  in comoving units. This is the first cosmic map, ever obtained, covering a  $> 100 \text{ Mpc}$  square area of the Universe at any high redshifts ( $z > 2$ ). In Figure 2, the LAEs have a very clumpy distribution, forming concentrations with a typical size of a few Mpc, comparable in size to the proto-cluster found by Venemans et al. (2002); Miley et al. (2004). These concentrations are not isolated, but connected with one another by filamentary overdense regions. The elongated overdense region of LAEs found by Shimasaku et al. (2003) at  $z = 4.86$  may be a segment of a descendant of such a filamentary structure. There are also found several voids of ellipsoidal shapes with sizes of  $10\text{--}40 \text{ Mpc}$  in which almost no galaxy exists. The characteristic sizes of filaments and voids seen in our map are comparable to those of the present-day Universe. Thus, this map marks the discovery of primeval LSSs at  $z = 5.7$ .

We quantify the large-scale clumpiness of the galaxy distribution by estimating  $\sigma_{20}$ , the rms fluctuation of galaxy overdensity within a sphere of  $20 \text{ Mpc}$  (comoving) radius. Considering that the radial depth of the surveyed volume is about  $40 \text{ Mpc}$ , we estimate the fluctuation by  $\sigma_{20}^2 \simeq \sigma_{\Sigma 20}^2 = [\langle (\Sigma_{20} - \bar{\Sigma}_{20})^2 \rangle - \bar{\Sigma}_{20}] / \bar{\Sigma}_{20}^2$ , where  $\sigma_{\Sigma 20}$  is the rms surface overdensity within circles of  $20 \text{ Mpc}$  radius, and  $\Sigma_{20}$  and  $\bar{\Sigma}_{20}$  are the observed number and the mean number of LAEs in a circle (Peebles 1980). We obtain  $\sigma_{20} = 0.4 \pm 0.2$ . This  $\sigma_{20}$  is comparable to or at least a half the value for the present-day LSSs, i.e.  $\sigma_{20}(z = 0) = 0.5 - 0.6$ , obtained from galaxies with  $b_j \leq 17.5$  (Seaborne et al. 1999). The characteristic shapes and the rms fluctuations indicate that these primeval LSSs at  $z \sim 6$  are similar to the present-day LSSs. We will present results of more detailed analyses for these primeval LSSs, such as counts-in-cell, in our forthcoming paper.

#### 3.2. Two Clumps Identified by Spectroscopy: Forming Clusters?

We find that among the dense concentrations seen in Figure 2, the one at  $2^h 17^m 47.2^s, -5^\circ 28' 40''$  [J2000] has the highest density contrast,  $\delta_{\Sigma} = 3.3$ , with the  $4.8\sigma$  significance level, where  $\delta_{\Sigma}$  is the surface overdensity for a circle of  $8 \text{ Mpc}$  radius. We refer to this concentration as Region A. Region B, a neighboring concentration at  $2^h 18^m 19.6^s, -5^\circ 32' 52''$  [J2000], also has a high density contrast of  $\delta_{\Sigma} = 1.5$  ( $2.2\sigma$ ). In order to obtain three-dimensional distributions of LAEs in Regions A and B, we carried out spectroscopy for LAEs with Subaru/FOCAS (Kashikawa et al. 2002) on 2003 December 20, 23, and 25. We placed a slit mask on each region. Another mask was put on a control field well separated from Regions A and B. We made a 2-hour exposure for each mask, and obtained 22 spectra in total, whose spectral range and resolution are  $\lambda = 4900\text{--}9400\text{\AA}$  and  $\lambda/\Delta\lambda \simeq 1000$ , respectively. Among the 22 objects, we classify one as an [OIII] emitter at  $z = 0.6$ , two as [OII] emitters at  $z = 1.2$ , and eight as securely identified LAEs with a characteristic asymmetric feature in Ly $\alpha$  line whose skewness exceeds 1.5 with the  $3\sigma$  level. We show spectra of these emitters in Figure 3. Since we have eight secure LAEs among the 11 ( $=8+2+1$ ) identified objects, we estimate the contamination rate of our LAE sample to be about 30%, which is consistent with those of other LAE samples (Rhoads et al. 2003; Shimasaku et al. 2003; Hu et al. 2004). The other 11 objects out of the 22 are emitters with an unresolved single line at  $\sim 8150\text{\AA}$ . Since most unresolved single line emitters have been found to be LAEs with a moderate velocity dispersion ( $\sim 200 \text{ km s}^{-1}$ ; Hu et al. 2004), we also regard these 11 objects as LAEs. Thus we have 19 LAEs with spectroscopic redshifts as summarized in Table 1.

We plot in Figure 4 the three-dimensional distribution of LAEs for Regions A and B. The histogram of Figure 4 shows that these regions have two clumps made of 10 LAEs with a significant excess. Each of the clumps has a diameter of about  $1 \text{ Mpc}$  in physical units ( $7 \text{ Mpc}$  in comoving units). For these clumps, the 1-dimensional velocity dispersion of galaxies is fairly small,  $\sim 180 \text{ km s}^{-1}$  (Clump A) and  $\sim 150 \text{ km s}^{-1}$  (B). Although these clumps may not be collapsed, the formal virial masses can be calculated from velocity dispersion,  $\sigma_{v1}$ , and radius,  $r$ , with  $3\sigma_{v1}^2 r / G$ , where  $G$  is the gravitational constant. We obtain  $\sim 1 \times 10^{13} M_{\odot}$  (Clump A) and  $\sim 8 \times 10^{12} M_{\odot}$  (B). The three-dimensional density contrast of LAEs,  $\delta_n = \delta n / \bar{n}$ , for the average of these clumps is  $\sim 80$ , which is comparable to those of present-day clusters,  $100 - 200$ . These clumps have the highest density in our surveyed volume of  $9 \times 10^5 \text{ Mpc}^3$  in comoving units. In the present-day Universe, this volume typically contains two massive clusters with mass of  $1 - 3 \times 10^{14} M_{\odot}$  (Reiprich & Böhringer 2002). Thus, the discovered clumps are likely proto-clusters which are ancestors of today's such clusters.

A particularly interesting feature is that these clumps are very high concentrations of star-forming galaxies with a star-formation rate of  $1 - 20 M_{\odot} \text{ yr}^{-1}$ . The star-formation rate density (SFRD) in these clumps inferred from Ly $\alpha$  fluxes is about 130 times higher than in the mean of the whole  $1 \text{ deg}^2$  field, mainly due to

a large overdensity,  $\delta_n \sim 80$ , of LAEs. This very high SFRD implies that these clumps would be just producing a number of galaxies in a short period by a burst of galaxy formation. In contrast, present-day massive clusters are dominated by old early-type galaxies, and show a deficit of young star-forming galaxies (Dressler 1980; Butcher & Oemler 1984). Since the formation epochs of early-type galaxies are estimated to be  $z = 2-5$  or earlier (e.g. Kodama, Arimoto, Barger, & Arag'on-Salamanca 1998), galaxies residing in these clumps are likely progenitors of the old early types seen in the core of present-day clusters. Therefore, we are probably witnessing forming clusters where a number of present-day early-type galaxies are just emerging as star-forming galaxies by a burst of galaxy formation.

### 3.3. Implications for Galaxy Formation

The Cold Dark Matter (CDM) model, the standard hierarchical scenario, predicts that very small initial fluctuations of mass density grow up gradually with time to evolve into galaxies and LSSs. However, the observed distribution of LAEs appears much more inhomogeneous than the dark-matter distribution, since the amplitude of the matter fluctuations at  $z = 5.7$  is predicted to be only 1/5 of the current value. If one wants to accept the CDM model, a solution to this discrepancy is to assume that LAEs are biased tracers of mass in a way to enhance the mass fluctuations. Previous observational studies of high- $z$  galaxies discuss the clustering bias (Adelberger et al. 1998; Giavalisco & Dickinson 2001; Ouchi et al. 2001; Shimasaku et al. 2004; Ouchi et al.

2004b). Theoretically, such biasing can be produced, if galaxies are formed at rare, highest peaks of yet small fluctuations of matter density (e.g. Mo & White 2002). From  $\sigma_{20}$ , we estimate that the bias parameter,  $b$ , the ratio of galaxy overdensity to matter overdensity, is  $b = 3.4 \pm 1.8$  on scales of LSSs (20 Mpc), which is comparable to the prediction at  $z \sim 5$  from simulations of galaxy formation based on the CDM model (Baugh et al. 1999; Kauffmann, Colberg, Diaferio, & White 1999). Thus, the CDM model may be consistent with the early formation of LSSs that we discovered, though the model needs to reproduce the characteristic shapes of observed LSSs, long filaments and large voids. On the other hand, we estimate the  $b$  value, in the CDM, which reproduces the observed number of forming clusters (two in  $9 \times 10^5$  Mpc<sup>3</sup>) with the size and the overdensity,  $\delta_n \sim 80$ , following the prescription of Shimasaku et al. (2003). We obtain  $b \sim 30$  for the two forming clusters, which is about ten times higher than the value for LSS scales, although this estimation of  $b$  is based on small statistics and might include a large error due to cosmic variance. This variety of  $b$  could be due to the dependence of  $b$  on the clustering scale or galaxy density (Benson et al. 2001). However, it is not yet clear how such a large difference in  $b$  may be produced within the framework of the CDM model. Our cosmic map may raise a question about how and where galaxies are formed in the early Universe.

M. Ouchi acknowledges the support from the Hubble Fellowship program through grant HF-01176.01-A.

### REFERENCES

- Adelberger, K. L., Steidel, C. C., Giavalisco, M., Dickinson, M., Pettini, M., & Kellogg, M. 1998, *ApJ*, 505, 18  
 Ajiki, M., et al. 2003, *AJ*, 126, 2091  
 Baugh, C. M., Benson, A. J., Cole, S., Frenk, C. S., & Lacey, C. G. 1999, *MNRAS*, 305, L21  
 Benson, A. J., Frenk, C. S., Baugh, C. M., Cole, S., & Lacey, C. G. 2001, *MNRAS*, 327, 1041  
 Bertin, E. & Arnouts, S. 1996, *A&AS*, 117, 393  
 Bruzual, G. & Charlot, S. 2003, *MNRAS*, 344, 1000  
 Butcher, H. & Oemler, A. 1984, *ApJ*, 285, 426  
 Coleman, G. D., Wu, C.-C., & Weedman, D. W. 1980, *ApJS*, 43, 393  
 Dressler, A. 1980, *ApJ*, 236, 351  
 Giavalisco, M. & Dickinson, M. 2001, *ApJ*, 550, 177  
 Gunn, J. E. & Stryker, L. L. 1983, *ApJS*, 52, 121  
 Hayashino, T., et al. 2003, *Publications of the National Astronomical Observatory of Japan*, 7, 33  
 Hu, E. M., Cowie, L. L., Capak, P., McMahon, R. G., Hayashino, T., & Komiyama, Y. 2004, *AJ*, 127, 563  
 Kashikawa, N. et al. 2002, *PASJ*, 54, 819  
 Kauffmann, G., Colberg, J. M., Diaferio, A., & White, S. D. M. 1999, *MNRAS*, 307, 529  
 Kinney, A. L., Calzetti, D., Bohlin, R. C., McQuade, K., Storchi-Bergmann, T., & Schmitt, H. R. 1996, *ApJ*, 467, 38  
 Kodama, T., Arimoto, N., Barger, A. J., & Arag'on-Salamanca, A. 1998, *A&A*, 334, 99  
 Kodama, T., et al. 2004, *MNRAS*, 350, 1005  
 Madau, P. 1995, *ApJ*, 441, 18  
 Miley, G. K., et al. 2004, *Nature*, 427, 47  
 Miyazaki, S. et al. 2002, *PASJ*, 54, 833  
 Mo, H. J. & White, S. D. M. 2002, *MNRAS*, 336, 112  
 Rhoads, J. E., et al. 2003, *AJ*, 125, 1006  
 Ouchi, M. et al. 2001, *ApJ*, 558, L83  
 Ouchi, M. et al. 2003, *ApJ*, 582, 60  
 Ouchi, M., et al. 2004a, *ApJ*, 611, 660  
 Ouchi, M., et al. 2004b, *ApJ*, 611, 685  
 Peebles, P. J. E. 1980, *The Large-Scale Structure of the Universe* (Princeton: Princeton Univ. Press)  
 Reiprich, T. H. & Böhringer, H. 2002, *ApJ*, 567, 716  
 Seaborne, M. D., et al. 1999, *MNRAS*, 309, 89  
 Sekiguchi, K. et al. 2004, *Astrophysics and Space Science Library*, 301, 169  
 Shimasaku, K. et al. 2003, *ApJ*, 586, L111  
 Shimasaku, K., et al. 2004, *ApJ*, 605, L93  
 Steidel, C. C., Adelberger, K. L., Dickinson, M., Giavalisco, M., Pettini, M., & Kellogg, M. 1998, *ApJ*, 492, 428  
 Steidel, C. C., Adelberger, K. L., Shapley, A. E., Pettini, M., Dickinson, M., & Giavalisco, M. 2000, *ApJ*, 532, 170  
 Venemans, B. P. et al. 2002, *ApJ*, 569, L11  
 Venemans, B. P., et al. 2004, *A&A*, 424, L17  
 Yagi, M., Kashikawa, N., Sekiguchi, M., Doi, M., Yasuda, N., Shimasaku, K., & Okamura, S. 2002, *AJ*, 123, 66

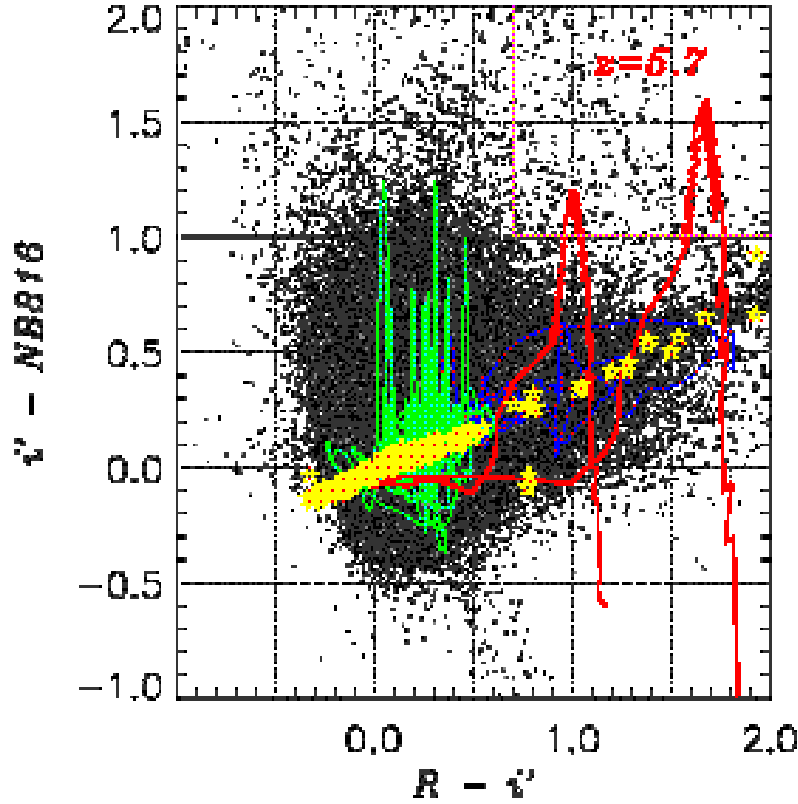


FIG. 1.— Two color diagrams for continuum color ( $R - i'$ ) and narrow-band excess color ( $i' - \text{NB816}$ ). The black dots indicate colors of 305,012 objects detected with  $\text{NB816} < 26.0$ . If the magnitude of an object is fainter than the  $1\sigma$  magnitude ( $1\sigma$  sky fluctuation), then the magnitude is replaced with the  $1\sigma$  magnitude. All the curves show colors of model galaxies at various redshifts. Red lines indicate model LAEs which are a composite spectrum of a 0.03 Gyr single burst model galaxy (GISSEL00; Bruzual & Charlot 2003) and a  $\text{Ly}\alpha$  emission ( $EW_0 = 22\text{\AA}$ ); from the left to right, two different amplitudes of inter-galactic medium absorption are applied:  $0.5\tau_{\text{eff}}$  and  $\tau_{\text{eff}}$ , where  $\tau_{\text{eff}}$  is Madau's (1995) median opacity. The narrow-band excess in each of the peaks in the red lines indicates the  $\text{Ly}\alpha$  emission of LAEs at  $z = 5.7$ . Green lines show 6 templates of nearby starburst galaxies (Kinney et al. 1996) up to  $z = 2$ , which are 6 classes of starburst galaxies with  $E(B - V) = 0.0 - 0.7$ . The narrow-band excess peaks in the green lines correspond to the emission lines of  $\text{H}\alpha$  ( $z = 0.2$ ),  $[\text{OIII}]$  ( $z = 0.6$ ),  $\text{H}\beta$  ( $z = 0.7$ ), or  $[\text{OII}]$  ( $z = 1.2$ ). Blue lines show colors of typical elliptical, spiral, and irregular galaxies (Coleman, Wu, & Weedman 1980) which are redshifted from  $z = 0$  to  $z = 3$ . Yellow star marks show 175 Galactic stars given by Gunn & Stryker (1983). The pink box surrounding the upper right region is the selection criteria of our  $z = 5.7$  LAEs. Because the distribution of the dots show a single track whose colors are consistent with that of the Galactic stars, our photometry is homogeneous over the  $1 \text{ deg}^2$  sky of the SXDF. **(The paper with high resolution images can be downloaded from [http://www-int.stsci.edu/~ouchi/work/astroph/sxds\\_LSS/](http://www-int.stsci.edu/~ouchi/work/astroph/sxds_LSS/))**

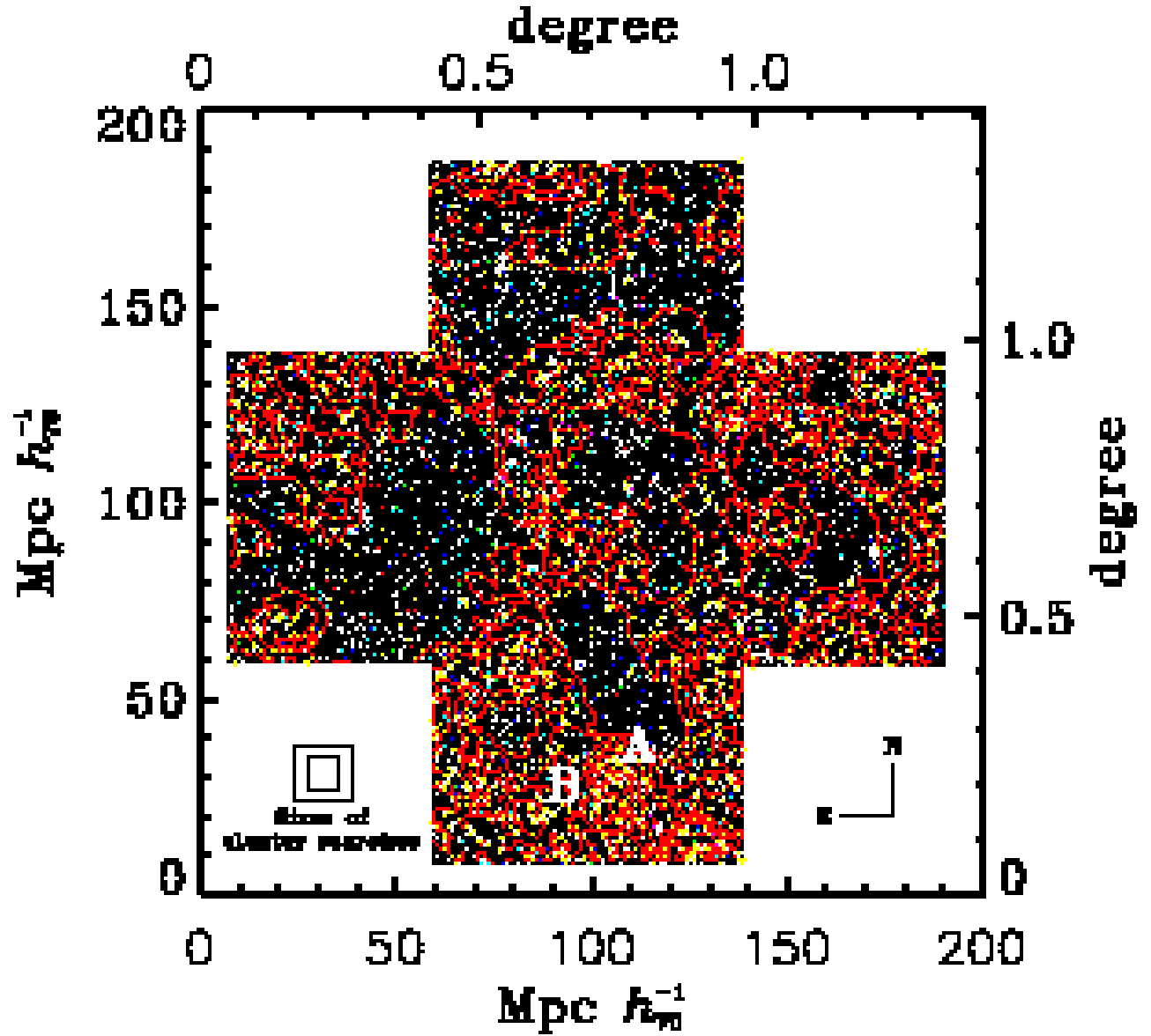


FIG. 2.— The distribution of  $z = 5.7 \pm 0.05$  LAEs in the SXDF. The positions of LAEs are shown with yellow dots. The red lines correspond to contours of galaxy overdensity from  $\delta_\Sigma = -0.25$  to  $3.25$  with a step of  $\Delta = 0.50$ . The characters, A and B, denote the positions of the two dense regions. The scale on the map is marked in both degrees and (comoving) megaparsecs. The large and small squares in the bottom left corner show the sizes of the surveyed areas in the previous proto-cluster searches by Venemans et al. (2002) and Miley et al. (2004), respectively. (The paper with high resolution images can be downloaded from [http://www-int.stsci.edu/~ouchi/work/astroph/sxds\\_LSS/](http://www-int.stsci.edu/~ouchi/work/astroph/sxds_LSS/))

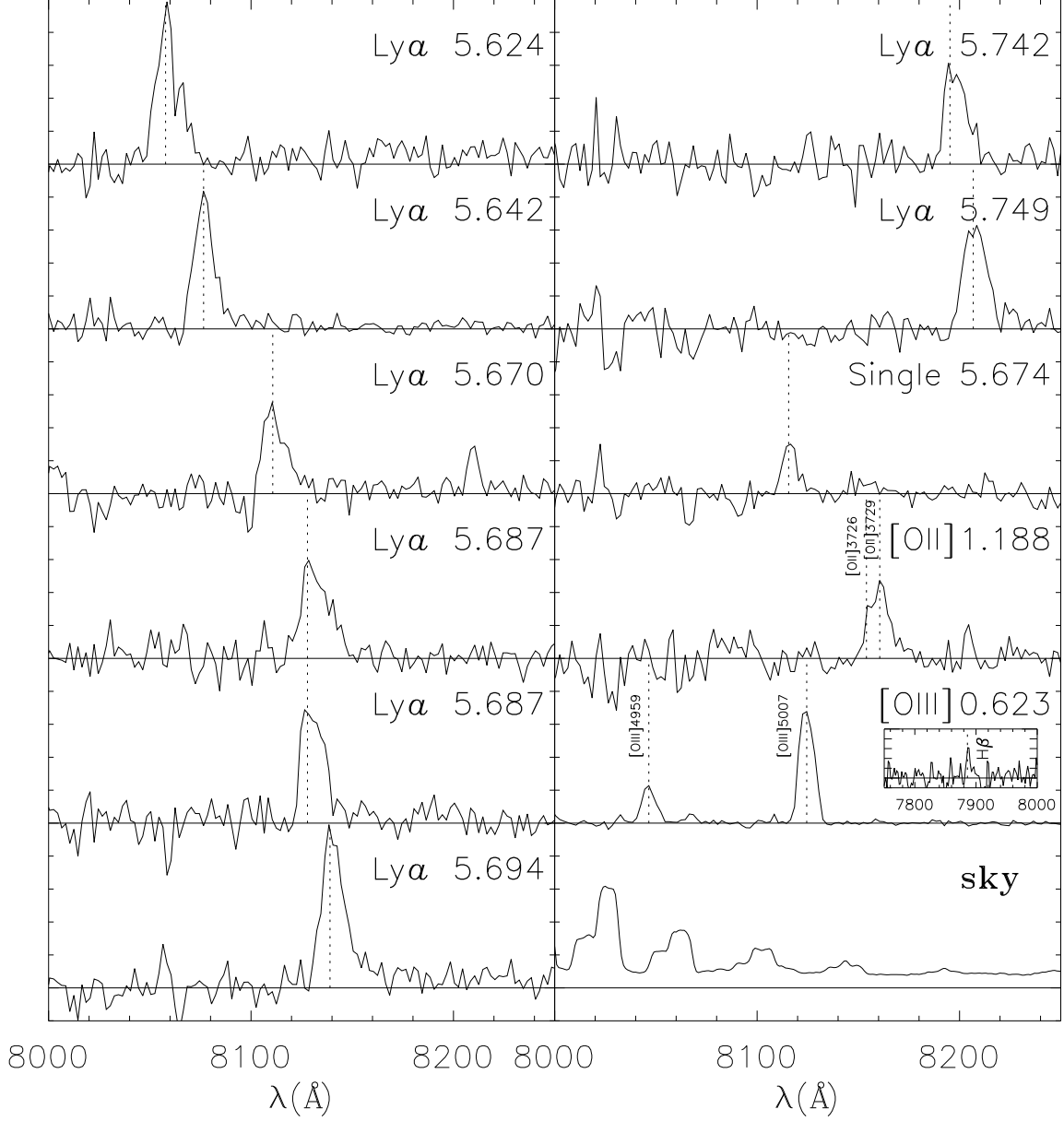


FIG. 3.— Spectra of eight secure LAEs, together with an unresolved-single line emitter and [OII] and [OIII] emitters. The caption on each panel indicates the classification and redshift. Ticks on the vertical axis denote  $3 \times 10^{-19} \text{ ergs s}^{-1} \text{ cm}^{-2} \text{ \AA}^{-1}$ , except for the following two panels because of display purpose. The second-top left and the fifth-top right panels have ticks of  $6 \times 10^{-19}$  and  $1.5 \times 10^{-18} \text{ ergs s}^{-1} \text{ cm}^{-2} \text{ \AA}^{-1}$ , respectively. The relative intensity of the night-sky emission is shown on the bottom right.

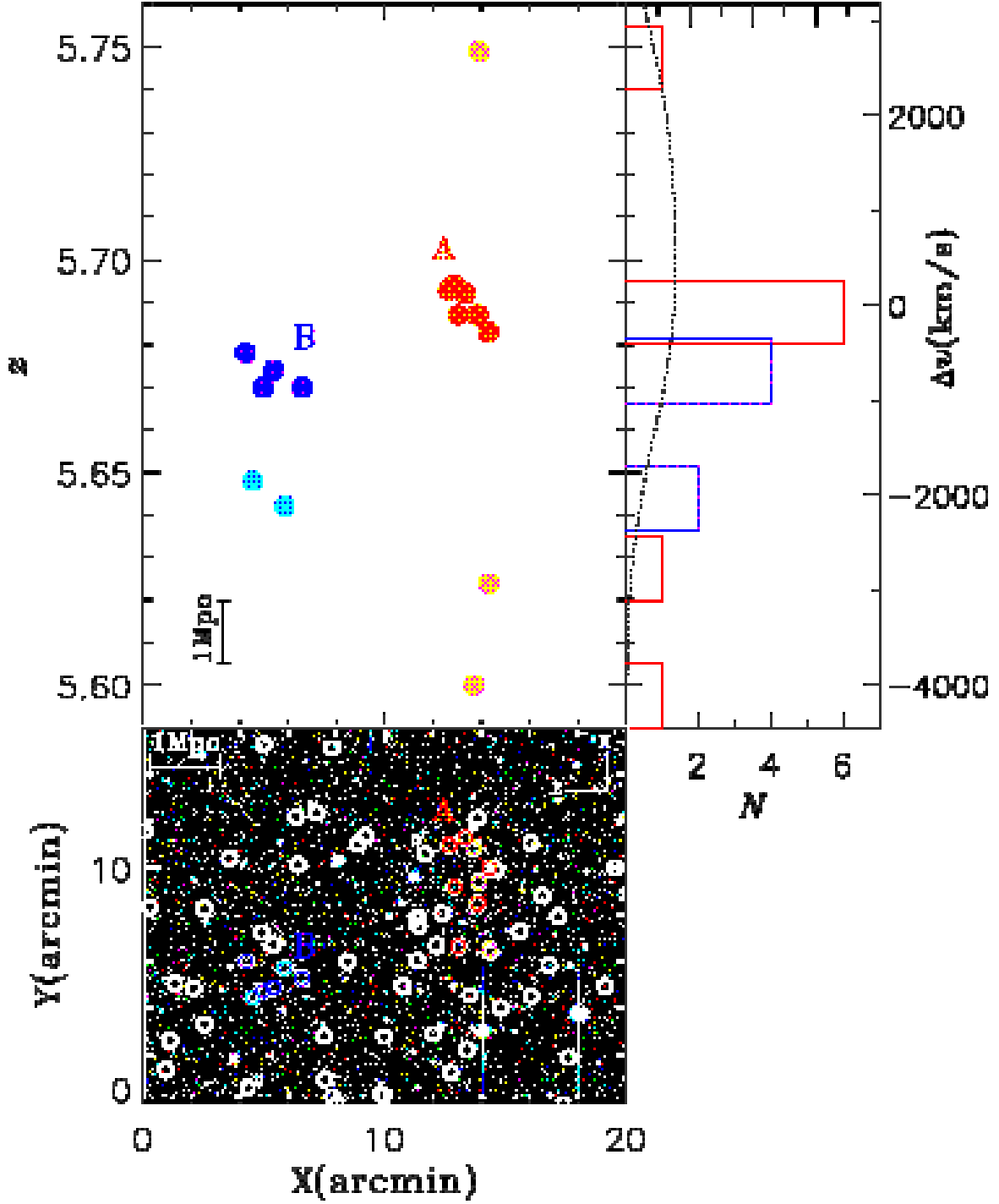


FIG. 4.— Three dimensional map of Regions A and B. The upper left panel shows the distribution of LAEs in transverse (East to the West) vs. radial (redshift) directions, while the bottom panel represents the distribution of LAEs projected on the sky. The red and blue circles correspond to the LAEs associated with the forming clusters (Clumps A and B), respectively, while the orange and cyan circles denote other LAEs in these regions. The white open circles plotted on the bottom panel denote the positions of LAEs without spectroscopic redshift. The vertical and horizontal bars indicate the length of 1 Mpc in physical units. The upper right panel shows the redshift distribution of LAEs with spectroscopic redshifts. The red and blue histograms correspond to LAEs in Regions A and B, respectively. The dotted line indicates the mean-expected number of LAEs for each region. (The paper with high resolution images can be downloaded from [http://www-int.stsci.edu/~ouchi/work/astroph/sxds\\_LSS/](http://www-int.stsci.edu/~ouchi/work/astroph/sxds_LSS/))

TABLE 1  
RESULTS OF SPECTROSCOPY

RA(J2000)	Dec(J2000)	$i'_{\text{AB}}$	$z$	$f$	$SFR$
02:17:45.03	-05:28:42.5	26.8	5.749 <sup>a</sup>	2.0	5.9
02:20:13.36	-04:51:09.3	26.7	5.742 <sup>a</sup>	1.3	3.7
02:20:26.14	-04:52:34.3	25.7	5.717	0.8	2.4
02:20:19.79	-04:52:29.9	26.4	5.706	1.0	2.9
02:17:49.13	-05:28:54.2	26.2	5.694 <sup>a</sup>	5.0	14.5
02:17:50.00	-05:27:08.2	27.4	5.693	0.7	1.9
02:17:47.32	-05:26:48.0	25.5	5.692	0.7	2.1
02:17:48.48	-05:31:27.0	26.6	5.687 <sup>a</sup>	1.4	3.9
02:17:45.27	-05:29:36.1	26.6	5.687 <sup>a</sup>	4.1	11.7
02:17:43.35	-05:28:07.1	26.2	5.683	7.0	20.0
02:18:23.82	-05:32:05.3	27.1	5.678	1.0	2.8
02:18:19.13	-05:33:11.7	27.1	5.674	2.0	5.7
02:18:20.88	-05:33:21.9	26.5	5.670	0.2	0.7
02:18:14.43	-05:32:49.1	26.5	5.670 <sup>a</sup>	1.0	2.9
02:20:21.52	-04:53:15.0	26.7	5.669	1.8	5.1
02:18:22.61	-05:33:37.8	27.6	5.648	1.5	4.4
02:18:17.35	-05:32:22.8	26.6	5.642 <sup>a</sup>	2.9	8.2
02:17:43.31	-05:31:35.0	26.5	5.624 <sup>a</sup>	2.5	7.1
02:17:45.88	-05:27:14.5	25.6	5.600	0.9	2.4
02:17:51.14	-05:29:35.3	27.2	1.188 <sup>b</sup>	1.7	...
02:20:12.15	-04:49:50.7	27.4	1.179 <sup>b</sup>	1.5	...
02:20:12.84	-04:50:22.5	24.5	0.623 <sup>c</sup>	11.9	...

NOTE. — The quantities  $i'_{\text{AB}}$ ,  $f$  and  $SFR$  are the  $i'$ -band magnitude measured in a  $2''$  diameter aperture, the total line flux in units of  $10^{-17}$  ergs  $s^{-1}$   $\text{cm}^{-2}$ , and the star-formation rate in units of  $M_{\odot}$   $\text{yr}^{-1}$ , respectively. The redshift,  $z$ , is measured from spectra summed over  $0''.9$  around the source center, while the line flux,  $f$ , is obtained from total flux falling in the slit.

<sup>a</sup>Securely identified LAEs

<sup>b</sup>[OII] emitters

<sup>c</sup>[OIII] emitter